Title

A Spinal Opsin Controls Early Neural Activity and Drives a Behavioral Light Response

Journal

Current Biology, 25(1)

ISSN

0960-9822

Authors

Friedmann, Drew
Hoagland, Adam
Berlin, Shai
et al.

Publication Date

2015

DOI

10.1016/j.cub.2014.10.055

Peer reviewed

Published in final edited form as:
Curr Biol. 2015 January 5; 25(1): 69–74. doi:10.1016/j.cub.2014.10.055.

A spinal opsin controls early neural activity and drives a behavioral light response

Drew Friedmann[1], **Adam Hoagland**[1], **Shai Berlin**, and **Ehud Y. Isacoff**[1,2,3,*]

[1]Dept. of Molecular and Cell Biology, UC Berkeley, Berkeley, CA 94720

[2]Helen Wills Neuroscience Institute, UC Berkeley, Berkeley, CA, 94720

[3]Physical Bioscience Division, Lawrence Berkeley National Laboratory, Berkeley, CA, 94720

Abstract

Non-visual detection of light by the vertebrate hypothalamus, pineal, and retina is known to govern seasonal and circadian behaviors [1]. However, the expression of opsins in multiple other brain structures [2–4] suggests a more expansive repertoire for light-regulation of physiology, behavior, and development. Translucent zebrafish embryos express extra-retinal opsins early on [5, 6], at a time when spontaneous activity in the developing central nervous system plays a role in neuronal maturation and circuit formation [7]. Though the presence of extra-retinal opsins is well documented, the function of direct photoreception by the central nervous system remains largely unknown. Here we show that early activity in the zebrafish spinal central pattern generator (CPG) and the earliest locomotory behavior are dramatically inhibited by physiological levels of environmental light. We find that the photo-sensitivity of this circuit is conferred by vertebrate ancient long opsin (VALopA), which we show to be a $G\alpha_i$-coupled receptor that is expressed in the neurons of the spinal network. Sustained photo-activation of VALopA not only suppresses spontaneous activity but also alters the maturation of time-locked correlated network patterns. These results uncover a novel role for non-visual opsins and a mechanism for environmental regulation of spontaneous motor behavior and neural activity in a circuit previously thought to be governed only by intrinsic developmental programs.

During the development of the nervous system, the first incidence of neural activity often occurs before sensory experience [7]. The frequency and pattern of this spontaneously generated activity guide neuronal differentiation, axon pathfinding, and synapse formation in many species and brain regions, including retina [8, 9], cortex [10, 11], hippocampus [12, 13], and spinal cord [14–17]. Since these activity networks are robust and stereotyped, we

*Correspondence to: ehud@berkeley.edu.

Author contributions: D.F. conceived the project. D.F. and E.Y.I. designed the experiments. Oocyte recordings and analysis were performed by S.B. Hardware and software were built and written by A.H. All other experiments were performed and analyzed by D.F. The manuscript was written by D.F. and E.Y.I. with input from S.B.

The authors declare no competing financial interests.

were surprised to find that spontaneous behavior, exhibited by embryonic zebrafish during the formation of its spinal central pattern generator (CPG), is heavily regulated by an unexpected external stimulus: light. Coiling behavior (Figure 1A and movie S1), a pre-locomotory behavior that is driven by spontaneous CPG activity [18, 19], was dramatically suppressed by illumination with green light (508 nm at 13.2 μW/mm^2) (Figure 1B). In dark-adapted fish at 22.5 hours post fertilization (hpf), coiling ceased within 1.7 ± 1.4 seconds of the start of illumination and the suppression persisted during a 2-minute period of constant illumination (Figure 1C and 1D, top). The light-induced suppression was also seen several hours later (27 hpf), but was preceded by a brief and transient phase of increased activity, as described recently [20] (Figure 1D, bottom). A systematic examination over early development revealed that photo-inhibition is present as soon as motor activity begins (Figure 1E and S1A).

Coiling was suppressed by light over a broad range of wavelengths, with a behavioral response λ_{max} at 504 nm (Figure 1F) and was inhibited by flashes of light as short as 70 msec (Figure 1G and S1E). The suppression lasted long after the termination of a light pulse, recovering to baseline dark-frequency over minutes ($t_{1/2}$ = 165 ± 21 seconds, *n* = 96) (Figure S1B). When illumination continued for minutes, the suppression of coiling partly adapted, relaxing to 43.0 ± 2.5% (*n* = 96) of the dark-adapted frequency (Figure S1C). Recovery from the light-adapted state also required minutes, similar to the recovery from a brief (2 sec) light-exposure (Figure S1C, D), demonstrating that the rate of recovery is independent of the extent of the inhibition and implying that the recovery from different light regimes engages similar signaling cascades. This also shows that the rapid freezing behavior is a genuine light-dependent response, rather than a non-specific reaction to an abrupt contrast change, such as the reversion to darkness following light adaptation (Figure S1C).

Since, at these early ages, zebrafish are blind because photoreceptors and retinal circuitry have not yet developed [21], we wondered if the photo-inhibition of coiling could reflect an intrinsic property of the CPG network. The nascent CPG resides entirely within the spinal cord, requiring putative pacemaker neurons in the most rostral somites, but not the hindbrain [22, 23]. We hypothesized that the calcium activity in the CPG network should therefore also be affected by light. Of the four earliest active cell types—ipsilateral-caudal projecting pacemakers (ICs), primary motor neurons (PMNs), ventral longitudinal descending interneurons (VeLDs), and sensory-driven contralaterally projecting ascending neurons (CoPAs)—the PMNs and VeLDs are contained within the 1020:Gal4 enhancer trap transgenic line [18, 22–26]. We used the genetically encoded calcium indicator GCaMP5 [27] to examine the effect of light on the activity of these cells (Figure 2A, left). To minimize potential photo-inhibition during calcium imaging, we excited GCaMP5 with 2-photon (2P) illumination at 920 nm. Under this condition, we observed spontaneous calcium events in 1020:Gal4$^+$ neurons at a frequency of 6.8 ± 0.7 events/min (*n* = 10 fish) (Figure 2A, black trace). The frequency was reduced by about half when excitation of GCaMP5 was switched to 1-photon (1P) illumination at 488 nm (3.6 ± 0.5 events/min; *n* = 10 fish) (Figure 2A, gray trace). Akin to the photo-inhibition of coiling behavior, neural activity at the end of the first day of development responded to a 5 sec stimulus of 561 nm light with a sustained reduction in the frequency of calcium events (e.g. 24 hpf Figure 2B and 2C), and the

inhibition was also induced by the blue-green portion of the visible spectrum (Figure 2D). Interestingly, ipsilateral correlation and contralateral alternation were not affected (Figure 2B and S2A), suggesting that acute light stimulation slows, rather than disrupts, natural behavior.

Detectable photo-inhibition of neural activity became evident at 20.5 hpf, shortly after activity in the network reaches its peak frequency (Figure 2C and S2B). As compared to photo-inhibition of coiling, the effect on neural activity appeared later and of smaller magnitude (compare with Figure 1E and S1A). These differences may arise from the methodological difference between whole-animal illumination, used to study coiling, and very localized illumination, as is done in GCaMP experiments. During Ca^{2+}-imaging, only somites 3–8 received the light stimulus—a fraction of the spinal cord, and missing the most mature, rostral portion of the spinal circuit. Nevertheless the photo-inhibition of neuronal activity by local illumination indicates that somites 3–8 of the spinal cord contain a light sensor that suppresses spontaneous activity.

Between 17 and 20 hpf, newly active neurons join into a circuit formed by ipsilaterally projecting interneurons and switch their pattern of activity from irregular, long, and isolated events to bursts of short events that are correlated among electrically coupled cells on the same side of the cord [18, 26]. By 22 hpf, most active 1020:$Gal4^+$ neurons have joined the CPG network, while a small group of cells display long-duration and uncorrelated activity [17, 26]. Previously, inhibition of early activity was shown to increase the fraction of the uncorrelated cells with long calcium events [26]. We found here that inhibiting activity before 20 hpf via global illumination with green light similarly resulted in a significantly higher percentage of active cells with long-duration, non-correlated calcium events at 22 hpf (Figure 2E, dashed area).

In an effort to identify genes whose protein products are involved in inhibition of the spinal CPG, we used fluorescence-activated cell sorting to purify fluorescent protein-expressing cells labeled by the UAS promoter when crossed to 1020:$Gal4^+$ fish (Figure S3A). Cells from trunk and tail samples of 20 hpf reporter fish were isolated, total RNA extracted, and RNAseq analysis performed [28]. We compared gene expression levels from the 1020:$Gal4^+$ subpopulation of neurons to those labeled in the pan-neuronal HuC:Gal4 line. Among the transcripts whose expression was elevated in 1020:$Gal4^+$ neurons was an extraretinal photoreceptor, namely vertebrate ancient long opsin A (VALopA), an evolutionary intermediate between invertebrate opsins and vertebrate visual photoreceptors [29]. Other genes with elevated expression in 1020:$Gal4^+$ neurons included known ventral spinal cord and motor neuron markers, as well as *olig2*, the genomic insertion site of the 1020:Gal4 enhancer trap [25] (Figure S3B, C). VALopA appeared to be a good candidate photoreceptor for inhibition of the spinal CPG based on its known presence in the spinal cord at 24 hpf and its previously described absorbance spectrum (λ_{max} = 510 nm) [5].

To test the hypothesis that VALopA is the photoreceptor mediating spinal CPG photo-inhibition, we used morpholino knockdown of VALopA expression [20]. The morpholino for VALopA, but not the scrambled control, completely abolished the inhibitory photoresponse in both young and older fish (Figure 3A–C and movie S2). At later ages,

when transient photo-excitation preceded photo-inhibition (Figure 3D), VALopA knockdown selectively abrogated the sustained photo-inhibition (Figure 3B). Thus, photo-inhibition develops concurrently with coiling, is elicited by spinal illumination alone, and requires VALopA. Conversely, photo-excitation develops later, is elicited by hindbrain illumination, and is independent of VALopA, in agreement with a recent report [20]. In order to determine whether photo-activation of VALopA in 1020:Gal4^{+} neurons is sufficient to drive inhibition, we mosaically expressed UAS-VALopA with a cerulean fluorescent marker in 1020:Gal4^{+} fish whose VALopA expression was knocked down by the splice-blocking morpholino. Photo-inhibition was seen only when the rescue construct was broadly expressed, and the degree of photo-inhibition increased with the expression level of the CFP marker, reporting higher expression levels of VALopA (Figure 3E, F).

To better understand the mechanism of photo-inhibition, we attempted to identify the intracellular signaling pathway that is activated by VALopA. We heterologously expressed zebrafish VALopA in *Xenopus laevis* oocytes and performed two-electrode voltage clamp recordings. Oocytes had no native light response, nor did injection of cRNA encoding VALopA on its own introduce a detectable light response (Figure 4A). However, co-injection of cRNAs encoding VALopA$_{GFP}$ and the neuronal G-protein activated inward rectifying potassium (GIRK) channel subunits (GIRK1$_{mCherry}$/GIRK2) (Figure S4A), yielded a large photo-current. Increasing external [K^{+}] from 2 to 24 mM generated an inward current (Figure 4A, B), as is typical of basal activation of GIRK by free native Gβγ in the oocyte [30]. Illumination with 535 nm light evoked an additional increase in current amplitude above basal level (Figure 4A, B and S4B), as is observed with ligand activation of the Gα$_{i}$ class of G protein coupled receptors (GPCRs), such as the acetylcholine-activated muscarinic-2 receptor m2R [31] (Figure S4D–F). Unlike activation of other GPCRs, the combined current persisted without decay for tens of seconds after the light was turned off (Figure 4A and S4B). Inward currents were blocked by the GIRK-channel blocker Ba^{2+}, further confirming that the light-induced currents are GIRK-mediated. These data suggest that VALopA is a Gα$_{i}$-coupled GPCR that turns off very slowly. In support of this, the photo-current was inhibited by expression of the specific Gα$_{i}$-inactivating pertussis toxin (PTX), even when co-expressed with additional wildtype Gα$_{i3}$ (Figure 4C, D). Moreover, PTX-insensitive Gα$_{i3}$ (C351I) [32] faithfully restored the photo-current in the presence of PTX (Figure 4C, D). As observed with the suppression of coiling behavior in zebrafish, GIRK current in oocytes could be triggered by very brief flashes of light (as short as 5 ms) and, as mentioned above, persisted for minutes afterwards in the dark (Figure S4C). Together, these findings indicate that VALopA couples to the Gα$_{i}$ pathway and suggest that the slow kinetics of this signaling can explain the kinetics of the light-induced inhibition of spontaneous activity and behavior in zebrafish.

Early optogenetics experiments demonstrated the ability of rat rhodopsin to couple to Gα$_{i}$ and inhibit spontaneously active networks in chick spinal cord [33]. We show that in fish, VALopA photo-inhibition similarly influences early activity before the onset of touch, sound, or visual responses, making it the earliest sensory input to the zebrafish spinal cord. At these early ages, spontaneous activity is an important developmental determinant before circuits, synapses, and cell fates are finalized [14–16, 26, 34, 35]. Whereas some activity-

dependent processes require competition between neurons, global activity levels were recently shown to regulate transmitter fate in *Xenopus* through the regulation of secreted brain-derived neurotrophic factor [35]. Indeed, we find that global photo-inhibition in early zebrafish affects the distribution of subsequent activity patterns in the locomotory CPG, perhaps reflecting a mechanism by which the light-dark cycle can sculpt early development. It is also conceivable, by analogy to the function of a VALopA homolog in ascidian larvae [36, 37] and an extraretinal photoreceptor in *Drosophila* larvae [38], that VALopA mediates a photosensitive avoidance behavior. At sunrise in the wild, embryos will be at varying stages of development, depending on spawning time and water temperature [39, 40]. The consistent inhibition by VALopA across these ages could drive a freezing behavior in bright light that eludes predators at a time when the embryo is trapped in the chorion and before sensory-evoked escape behavior emerges. The uneven timing of development and sunrise could also affect activity-driven processes in an age-dependent fashion, but it is unknown if this would diversify or synchronize the relationship between development and the photoperiod. It will be interesting to see if spontaneously active circuits in other brain regions are similarly flexible to environmental regulation and also if non-visual opsins can acutely control behavior in other vertebrates.

Supplementary Material

Refer to Web version on PubMed Central for supplementary material.

Acknowledgments

We thank H. Nolla and the Berkeley Flow Cytometry Core for assistance with FACS, Y. G. Choi, J. Ngai and the Berkeley Functional Genomics Laboratory for assistance and guidance with RNA-Seq. This work used the Vincent J. Coates Genomics Sequencing Laboratory at UC Berkeley, supported by NIH S10 Instrumentation Grants S10RR029668 and S10RR027303. We also thank D. Kojima (University of Tokyo, Japan) for providing VALopA cDNA, N. Dascal (Tel Aviv University, Israel) for providing GIRK1, GIRK2, and $G\alpha_{i3}$, E. Reuveny (Weizmann Institute, Israel) for providing PTX-S1, and L. Looger (Janelia Farm) for making GCaMP5 available. This work was supported by the National Institutes of Health Nanomedicine Development Center for the Optical Control of Biological Function (2PN2EY01824). RNA-seq .fastq files can be found via the Gene Expression Omnibus archive, accession number (placeholder)######.

References and Notes

1. Peirson SN, Halford S, Foster RG. The evolution of irradiance detection: melanopsin and the non-visual opsins. Philos Trans R Soc Lond, B, Biol Sci. 2009; 364:2849–2865. [PubMed: 19720649]
2. Fernandes AM, Fero K, Driever W, Burgess HA. Enlightening the brain: linking deep brain photoreception with behavior and physiology. Bioessays. 2013; 35:775–779. [PubMed: 23712321]
3. Cheng N, Tsunenari T, Yau KW. Intrinsic light response of retinal horizontal cells of teleosts. Nature. 2009; 460:899–903. [PubMed: 19633653]
4. Nissilä J, Mänttäri S, Särkioja T, Tuominen H, Takala T, Timonen M, Saarela S. Encephalopsin (OPN3) protein abundance in the adult mouse brain. J Comp Physiol A. 198:833–839.
5. Kojima D, Torii M, Fukada Y, Dowling JE. Differential expression of duplicated VAL-opsin genes in the developing zebrafish. J Neurochem. 2008; 104:1364–1371. [PubMed: 18036148]
6. Fernandes AM, Fero K, Arrenberg AB, Bergeron SA, Driever W, Burgess HA. Deep brain photoreceptors control light-seeking behavior in zebrafish larvae. Curr Biol. 2012; 22:2042–2047. [PubMed: 23000151]
7. Kirkby LA, Sack GS, Firl A, Feller MB. A role for correlated spontaneous activity in the assembly of neural circuits. Neuron. 2013; 80:1129–1144. [PubMed: 24314725]

8. Ackman JB, Burbridge TJ, Crair MC. Retinal waves coordinate patterned activity throughout the developing visual system. Nature. 2012; 490:219–225. [PubMed: 23060192]
9. Penn AA, Riquelme PA, Feller MB, Shatz CJ. Competition in retinogeniculate patterning driven by spontaneous activity. Science. 1998; 279:2108–2112. [PubMed: 9516112]
10. Garaschuk O, Linn J, Eilers J, Konnerth A. Large-scale oscillatory calcium waves in the immature cortex. Nat Neurosci. 2000; 3:452–459. [PubMed: 10769384]
11. Yu YC, He S, Chen S, Fu Y, Brown KN, Yao XH, Ma J, Gao KP, Sosinsky GE, Huang K, et al. Preferential electrical coupling regulates neocortical lineage-dependent microcircuit assembly. Nature. 2012; 486:113–117. [PubMed: 22678291]
12. Kleindienst T, Winnubst J, Roth-Alpermann C, Bonhoeffer T, Lohmann C. Activity-dependent clustering of functional synaptic inputs on developing hippocampal dendrites. Neuron. 2011; 72:1012–1024. [PubMed: 22196336]
13. Ben-Ari Y, Cherubini E, Corradetti R, Gaiarsa JL. Giant synaptic potentials in immature rat CA3 hippocampal neurones. J Physiol (Lond). 1989; 416:303–325. [PubMed: 2575165]
14. Kastanenka KV, Landmesser LT. In vivo activation of channelrhodopsin-2 reveals that normal patterns of spontaneous activity are required for motoneuron guidance and maintenance of guidance molecules. J Neurosci. 2010; 30:10575–10585. Available at: http://www.jneurosci.org/content/30/31/10575.full.pdf+html. [PubMed: 20686000]
15. Plazas PV, Nicol X, Spitzer NC. Activity-dependent competition regulates motor neuron axon pathfinding via PlexinA3. Proc Natl Acad Sci USA. 2013; 110:1524–1529. [PubMed: 23302694]
16. Pineda RH, Svoboda KR, Wright MA, Taylor AD, Novak AE, Gamse JT, Eisen JS, Ribera AB. Knockdown of Nav1.6a Na+ channels affects zebrafish motoneuron development. Development. 2006; 133:3827–3836. [PubMed: 16943272]
17. Gu X, Olson EC, Spitzer NC. Spontaneous neuronal calcium spikes and waves during early differentiation. J Neurosci. 1994; 14:6325–6335. [PubMed: 7965039]
18. Saint-Amant L, Drapeau P. Synchronization of an embryonic network of identified spinal interneurons solely by electrical coupling. Neuron. 2001; 31:1035–1046. Available at: http://ac.els-cdn.com/S0896627301004160/1-s2.0-S0896627301004160-main.pdf?_tid=891ffe68-d0b2-11e3-a7a6-00000aab0f27&acdnat=1398895277_d181361d1681059bc4cfc47b8a620394. [PubMed: 11580902]
19. Saint-Amant L. Development of motor rhythms in zebrafish embryos. Prog Brain Res. 2010; 187:47–61. [PubMed: 21111200]
20. Kokel D, Dunn TW, Ahrens MB, Alshut R, Cheung CYJ, Saint-Amant L, Bruni G, Mateus R, van Ham TJ, Shiraki T, et al. Identification of nonvisual photomotor response cells in the vertebrate hindbrain. J Neurosci. 2013; 33:3834–3843. [PubMed: 23447595]
21. Chhetri J, Jacobson G, Gueven N. Zebrafish--on the move towards ophthalmological research. Eye (Lond). 2014; 28:367–380. [PubMed: 24503724]
22. Pietri T, Manalo E, Ryan J, Saint-Amant L, Washbourne P. Glutamate drives the touch response through a rostral loop in the spinal cord of zebrafish embryos. Dev Neurobiol. 2009; 69:780–795. [PubMed: 19634126]
23. Tong H, McDearmid JR. Pacemaker and plateau potentials shape output of a developing locomotor network. Curr Biol. 2012; 22:2285–2293. [PubMed: 23142042]
24. Scott EK, Mason L, Arrenberg AB, Ziv L, Gosse NJ, Xiao T, Chi NC, Asakawa K, Kawakami K, Baier H. Targeting neural circuitry in zebrafish using GAL4 enhancer trapping. Nat Meth. 2007; 4:323–326.
25. Wyart C, Del Bene F, Warp E, Scott EK, Trauner D, Baier H, Isacoff EY. Optogenetic dissection of a behavioural module in the vertebrate spinal cord. Nature. 2009; 461:407–410. [PubMed: 19759620]
26. Warp E, Agarwal G, Wyart C, Friedmann D, Oldfield CS, Conner A, Del Bene F, Arrenberg AB, Baier H, Isacoff EY. Emergence of patterned activity in the developing zebrafish spinal cord. Curr Biol. 2012; 22:93–102. [PubMed: 22197243]
27. Akerboom J, Chen TW, Wardill TJ, Tian L, Marvin JS, Mutlu S, Calderón NC, Esposti F, Borghuis BG, Sun XR, et al. Optimization of a GCaMP calcium indicator for neural activity imaging. J Neurosci. 2012; 32:13819–13840. [PubMed: 23035093]

28. Ferreira T, Wilson SR, Choi YG, Risso D, Dudoit S, Speed TP, Ngai J. Silencing of odorant receptor genes by G protein βγ signaling ensures the expression of one odorant receptor per olfactory sensory neuron. Neuron. 2014; 81:847–859. [PubMed: 24559675]
29. Sato K, Yamashita T, Ohuchi H, Shichida Y. Vertebrate Ancient-Long Opsin Has Molecular Properties Intermediate between Those of Vertebrate and Invertebrate Visual Pigments. Biochemistry. 2011; 50:10484–10490. [PubMed: 22066464]
30. Reuveny E, Slesinger PA, Inglese J, Morales JM, Iñiguez-Lluhi JA, Lefkowitz RJ, Bourne HR, Jan YN, Jan LY. Activation of the cloned muscarinic potassium channel by G protein beta gamma subunits. Nature. 1994; 370:143–146. [PubMed: 8022483]
31. Lüscher C, Slesinger PA. Emerging roles for G protein-gated inwardly rectifying potassium (GIRK) channels in health and disease. Nat Rev Neurosci. 2010; 11:301–315. [PubMed: 20389305]
32. West RE, Moss J, Vaughan M, Liu T, Liu TY. Pertussis toxin-catalyzed ADP-ribosylation of transducin. Cysteine 347 is the ADP-ribose acceptor site. J Biol Chem. 1985; 260:14428–14430. [PubMed: 3863818]
33. Li X, Gutierrez DV, Hanson MG, Han J, Mark MD, Chiel H, Hegemann P, Landmesser LT, Herlitze S. Fast noninvasive activation and inhibition of neural and network activity by vertebrate rhodopsin and green algae channelrhodopsin. Proc Natl Acad Sci USA. 2005; 102:17816–17821. [PubMed: 16306259]
34. Crisp SJ, Evers JF, Bate M. Endogenous patterns of activity are required for the maturation of a motor network. J Neurosci. 2011; 31:10445–10450. [PubMed: 21775590]
35. Guemez-Gamboa A, Xu L, Meng D, Spitzer NC. Non-Cell-Autonomous Mechanism of Activity-Dependent Neurotransmitter Switching. Neuron. 2014; 82:1004–1016. [PubMed: 24908484]
36. Kusakabe T, Kusakabe R, Kawakami I, Satou Y, Satoh N, Tsuda M. Ci-opsin1, a vertebrate-type opsin gene, expressed in the larval ocellus of the ascidian Ciona intestinalis. FEBS Lett. 2001; 506:69–72. [PubMed: 11591373]
37. Inada K, Horie T, Kusakabe T, Tsuda M. Targeted knockdown of an opsin gene inhibits the swimming behaviour photoresponse of ascidian larvae. Neurosci Lett. 2003; 347:167–170. [PubMed: 12875912]
38. Xiang Y, Yuan Q, Vogt N, Looger LL, Jan LY, Jan YN. Light-avoidance-mediating photoreceptors tile the Drosophila larval body wall. Nature. 2010; 468:921–926. [PubMed: 21068723]
39. Spence R, Ashton R, Smith C. Oviposition decisions are mediated by spawning site quality in wild and domesticated zebrafish, Danio rerio. Behaviour. 2007; 144:953–966.
40. Engeszer RE, Patterson LB, Rao AA, Parichy DM. Zebrafish in the wild: a review of natural history and new notes from the field. Zebrafish. 2007; 4:21–40. [PubMed: 18041940]

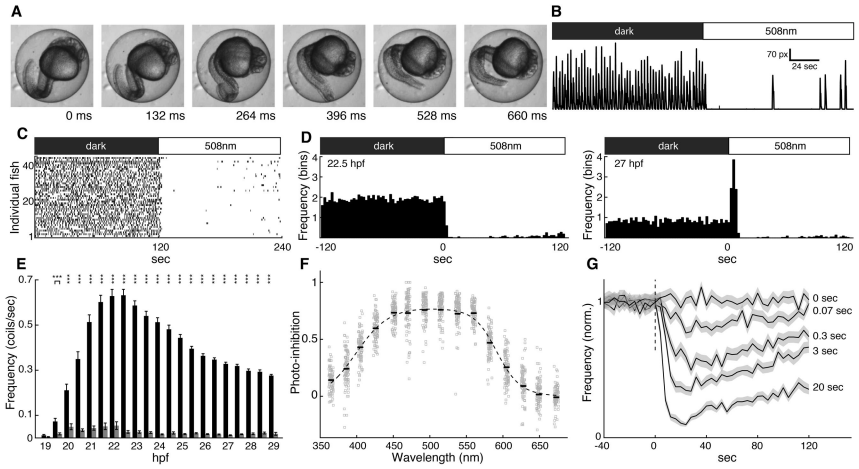

Figure 1.

Effect of light on frequency of spontaneous coiling behavior. **A.** Still frames from a movie of a single spontaneous coil in a 27 hpf embryo. **B.** Trace of detected motion (pixel changes) from video of an individual embryo before (dark) and during (508 nm) illumination; peaks represent individual coiling events. **C.** Raster plot of coiling events measured simultaneously in 44 dark-adapted 22.5 hpf embryos under dark and light conditions. **D.** Left, peri-stimulus time histogram of 22.5 hpf embryos from data in (C). Right, histogram of the same fish at 27 hpf. Frequency = mean coils/fish within bins of 2.4 sec. **E.** Mean baseline coiling frequencies (coils/sec) in the dark (black bars) and under green light (gray bars) over developmental time. Two-tailed paired *t* test with Bonferroni adjusted p-values, *** $p < 0.001$; $n = 39–75$. **F.** Photo-inhibition $[-(Hz_{Light}-Hz_{Dark})/Hz_{Dark}$; coiling measured over 120 sec in each condition] as a function of wavelength. Gray squares are individual responses < 3 s.d. from each mean (black lines). Light power = 133–159 nW/mm^2; $n = 96$. **G.** Photo-inhibition of coiling frequency by light flashes of indicated durations. Lines indicate normalized mean, bins = 4 sec; s.e.m. in grey; $n = 96$.

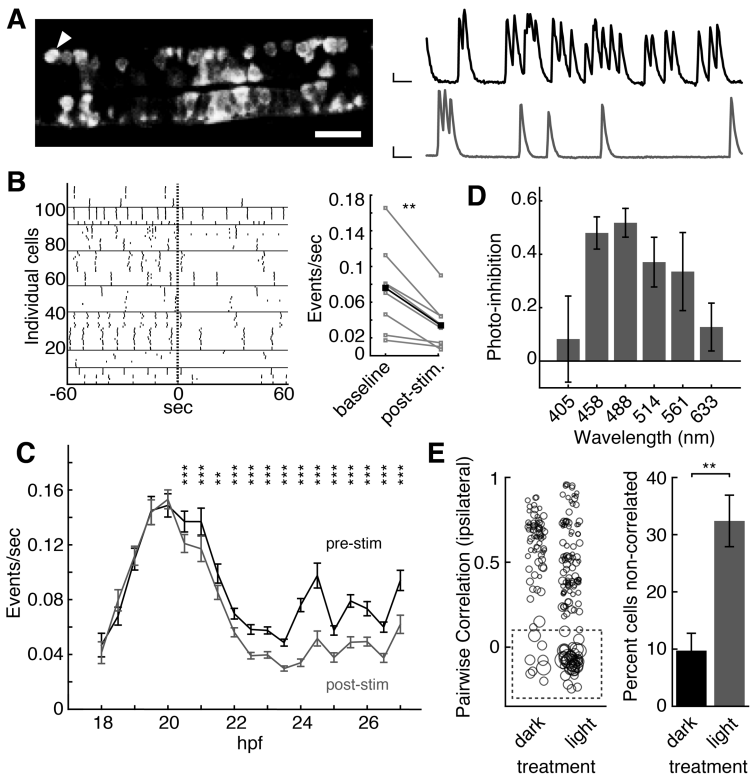

Figure 2.

Acute and delayed effects of light on neural activity. **A.** Left, image of GCaMP5 fluorescence in ventral spinal cord somites 3–8 of a 1020:Gal4; UAS:GCaMP5 embryo. Scale bar = 20 μm. Right, calcium traces from one cell (arrowhead in image) under 2P (black trace, 920 nm) or subsequent period of 1P (gray trace, 488 nm) excitation, following < 5 sec interval. Axes: 100% ΔF/F, 10 sec. **B.** Left, raster plot of 2P-imaged calcium events in 24 hpf embryos before and after a 5 sec flash (dashed line) with 561 nm light. Measurements from each of 8 fish (horizontal lines delineate individual fish). Right, quantification of calcium event frequency in the 8 fish (grey lines; mean = black line) during a 180 sec period under 2P excitation (baseline) and over 60 sec following the 561 nm light flash (post-stim.). Two-tailed paired *t* test $p < 0.01$. **C.** Frequency of calcium events over 9 hours of development measured under 2P excitation before (pre-stim) and after (post-stim.) a 5 sec 561 nm light flash, as quantified in (B). Two-tailed paired *t* test, Bonferroni adjusted p-values, *** $p < 0.001$, ** $p < 0.01$; *n* = 21–123 cells from 4–8 fish at each age. **D.** Photo-inhibition after illumination with a 5 sec light flash at varying wavelengths. 103–110 μW/pixel; *n* = 16 cells in 8 fish at each wavelength. **E.** Left, pairwise ipsilateral correlations between cells in 22 hpf embryos following dark or light (508 nm, 13.2 $\mu W/mm^2$) rearing for 2 hours before 20 hpf. Circle size proportional to event width at half max amplitude (range = 1.8–75.7 sec). Dashed box demarcates non-correlated cells. Right, percentage of non-correlated cells (ipsilateral correlation < 0.1) at 22 hpf. Two-tailed unpaired *t* test, $p = 0.004$. *n* = 6 (dark) and 8 fish (light).

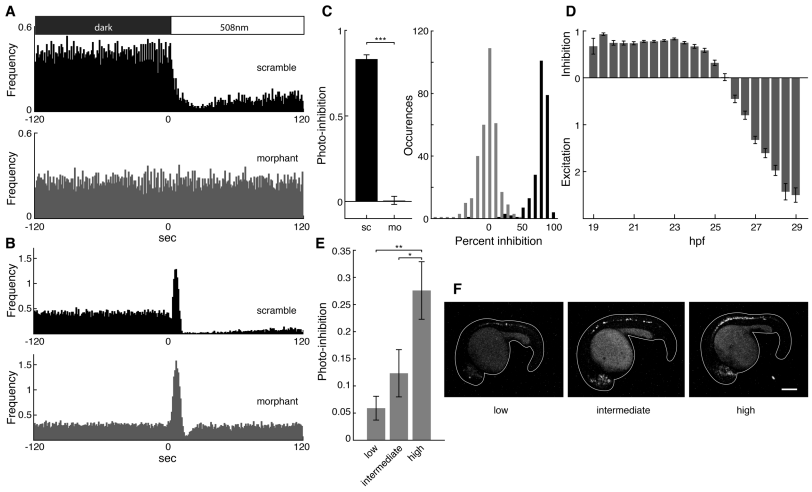

Figure 3.

Light inhibition of coiling depends on an extraretinal opsin. **A,B.** Representative peri-stimulus time histograms of coiling frequency (events/sec; mean across 6 trials; bin = 1 sec) of embryos at 22–25 hpf (A) or 27–31 hpf (B). Zygotes injected with scrambled control morpholino (*n* = 23 in (A), 34 in (B)) (black) or morpholino against VALopA (*n* = 24 in (A), 41 in (B)) (gray). **C.** Left, mean photo-inhibition of scrambled control morpholino (sc; *n* = 40) and morpholino (mo; *n* = 55) injected 22–25 hpf embryos. Two-tailed unpaired *t* test, $p < 0.001$. Right, frequency distribution of percent photo-inhibition (6 responses per fish) in scrambled control morpholino embryos (black) and morpholino embryos (gray). **D.** Normalized inhibition or excitation of coiling frequency $[-(Hz_{Light}-Hz_{Dark})/Hz_{Dark}]$ in first 12 sec after light onset relative to a 120 sec preceding baseline in darkness (*n* = 39–75). **E.** Mean photo-inhibition (5 responses per fish) of morpholino-injected embryos mosaically expressing low, intermediate, or high levels of a VALopA rescue construct with a mCerulean marker. One-way ANOVA with Tukey *post hoc* analysis, * $p < 0.05$, ** $p < 0.01$; *n* = 59 (low), 18 (intermediate), and 11 (high). **F.** Images of representative embryos expressing low, intermediate, and high levels of mCerulean fluorescence. Scale bar = 200 μm.

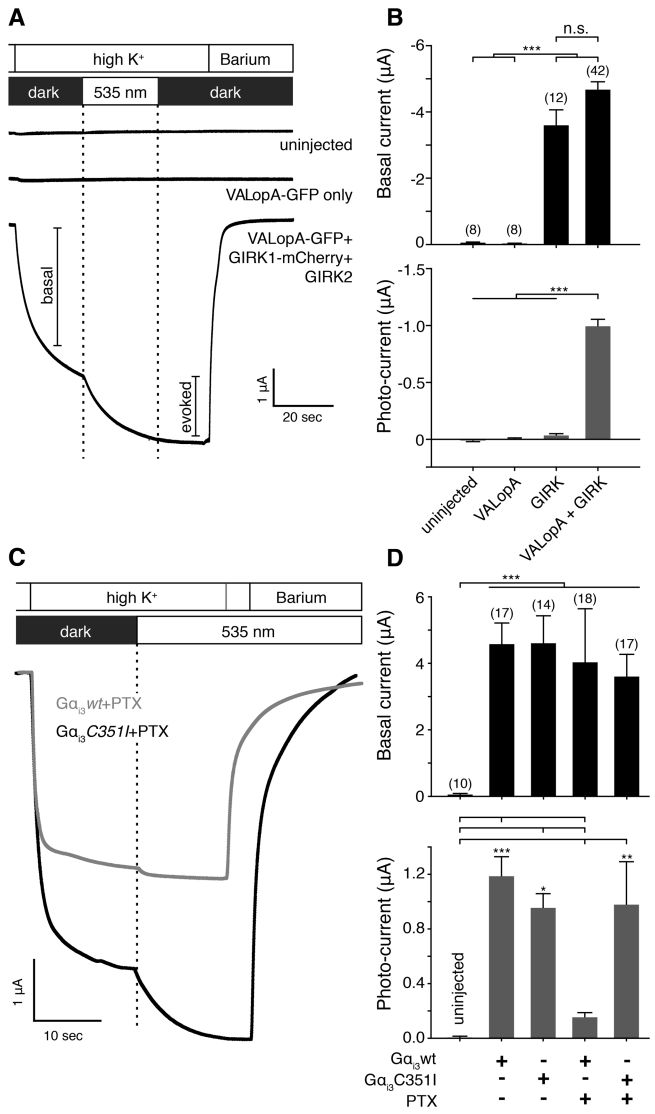

Figure 4.

VALopA couples to $Ga_{i/o}$ in *Xenopus* oocytes. **A.** Representative voltage clamp currents from an uninjected oocyte (top trace), an oocyte expressing zebrafish $VALopA_{GFP}$ alone (middle trace), or co-expressing $VALopA_{GFP}$ with $GIRK1_{mCherry}$ and GIRK2. Oocytes are initially bathed in ND96, switches to 24 mM K^+ (high K^+), and then 5 mM Ba^{2+} in 24 mM K^+ (Barium). Illumination through a 535/50 nm bandpass filter (~70 mW/mm^2) is indicated. **B.** Summary for the basal (top) and light-evoked (bottom) GIRK currents as in (A). **C.** Representative currents (protocols as in (A)) from oocytes expressing $VALopA_{GFP}$, $GIRK1_{mCherry}$ and GIRK2 with the catalytic subunit of pertussis toxin, (PTX-S1) and either PTX-sensitive $G\alpha_{i3}$-*wt* (gray) or PTX-insensitive C351I mutant $G\alpha_{i3}$ (black). **D.** Summary for the basal (top) and light-evoked (bottom) GIRK currents in oocytes expressing combinations of $G\alpha_{i3}$-*wt*, $G\alpha_{i3}$-C351I, and PTX. One-way ANOVA with Tukey *post hoc* analysis * $p < 0.05$, ** $p < 0.01$, *** $p < 0.001$; *n* is indicated above bars.